

## Vehicle Tests of a Longitudinal Control Law for Application to Stop-and-Go Cruise Control

Ilki Moon

*Department of Automotive Engineering, Hanyang University, Seoul 133-791, Korea*

Kyongsu Yi\*

*School of Mechanical Engineering, Hanyang University, Seoul 133-791, Korea*

This paper presents the implementation and vehicle tests of a vehicle longitudinal control scheme for Stop and Go cruise control. The control scheme consists of a vehicle-to-vehicle distance control algorithm and throttle/brake control algorithm for acceleration tracking. The desired acceleration of a vehicle for vehicle-to-vehicle distance control has been designed using Linear Quadratic optimal control theory. Performance of the control algorithm has been investigated via vehicle tests. A millimeter wave radar sensor has been used for distance measurement. A stepper motor and an electronic vacuum booster have been used for throttle/brake actuators, respectively. It has been shown that the proposed control algorithm can provide satisfactory performance.

**Key Words :** Vehicle Longitudinal Control, Throttle, Brake, Distance Control, Optimal Control, Vehicle

### 1. Introduction

Researches on vehicle longitudinal control for applications to Automated Highway Systems (AHS) have been in progress for several decades (Fenton et al, 1969 ; Rajamani et al, 1998; Shladover, 1978). Driver assistant systems have been an active topic of research and development since the 1990's due to the potential for improved driving comfort and increased vehicle safety. Driver assistant systems currently under development by most automotive manufacturers around the world and recently commercialized by several companies are Adaptive Cruise Control (ACC) and Stop and Go (S&G) cruise control systems. The goal of S&G is the partial automation of the longitudinal vehicle control and the reduction of the workload of the driver, with the aim to

support and relieve the driver in a convenient manner on the busy urban traffic way. ACC and S&G systems control both speed and distance to forward vehicles, and can both improve driving comfort and reduce the danger of rear-end-collisions. Vehicles with S&G can follow other cars in dense traffic while keeping a safe distance in stop and go driving situations.

The basic requirements for realizing an S&G cruise control system have been discussed by Venhovens et al. Since the bandwidth of an ACC vehicle is very low and the clearance (the vehicle-to-vehicle distance) is large, the powertrain dynamics of a vehicle have insignificant impact on the performance of the vehicle acceleration control. In the case of stop and go driving situations, the bandwidth of the longitudinal vehicle control system should be increased significantly to reduce the clearance and to be meaningful on the busy urban traffic highway. Since the speed ratio of the torque converter pump and turbine speeds changes significantly in the case of stop and go driving, the throttle/brake control laws must be designed taking into account the vehicle

---

\* Corresponding Author,

E-mail : kyongsu@hanyang.ac.kr

TEL : +82-2-2290-0455; FAX : +82-2-2296-0561

School of Mechanical Engineering, Hanyang University, Seoul 133-791, Korea. (Manuscript Received October 30, 2001; Revised June 10, 2002)

powertrain and brake system dynamics.

Although Stop and Go is no longer limited to the simple task of following a vehicle immediately in front of the S&G vehicle, vehicle-to-vehicle distance control is one of the key features of the S&G systems. The brake and throttle controls should be gently applied so that the driver feels comfortable and is not surprised by the control actions, while the speed control error and the errors between the desired headway distance and the actual vehicle-to-vehicle distance are kept within acceptable limits. A vehicle speed and vehicle-to-vehicle distance control algorithm for a vehicle S&G system has been proposed in this paper. The control algorithm consists of speed and distance control algorithms and a combined throttle/brake control law. Linear Quadratic (LQ) optimal control theory has been used to design a vehicle desired acceleration for vehicle-to-vehicle distance control. The engine throttle control law has been designed taking into account the torque converter dynamics.

## 2. Vehicle Longitudinal Control System

Figure 1 shows a vehicle longitudinal control system. The system consists of a radar sensor, a controller (ECU), a brake actuator and a throttle actuator.

Vehicle longitudinal control algorithms have been studied extensively for applications to vehicle intelligent cruise control and automated highways in the last decade (Chang, 1994; Chien et al., 1994; Choi et al., 1995; Fujioka et al., 1995; Germann et al., 1995; Hedrick et al., 1991; Hedrick et al., 1993; Hoess et al., 1996; Ioannou et al., 1993; Winner et al., 1996; Yi et al., 2001). The torque converter plays an important role in the stop-and-go driving situations and should

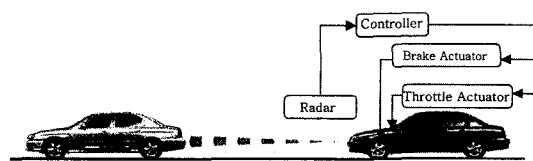


Fig. 1 Vehicle longitudinal control system

be accounted for the development of the throttle/brake control law.

The main task of the S&G controller is to translate the desired behavior resulting from the situation and treat assessment into appropriate throttle/brake control actions so that the vehicle speed and the headway distance track the desired values. Figure 2 shows a block diagram of the vehicle longitudinal control algorithm for application to S&G cruise control. The control algorithm consists of a set-speed-control algorithm, a speed-control algorithm, a distance-control algorithm and a combined throttle/brake control law. Time gap and set speed are the inputs to the controller from the driver. If there is no vehicle in front of the subject vehicle, the controller activates throttle/brake actuators based on the set-speed-control algorithm. When a forward vehicle is detected, the controller uses either the speed-control algorithm or distance-control algorithm depending on the detected vehicle-to-vehicle distance, i.e., the clearance. If the current actual clearance,  $c_{act}$ , is greater than the transition distance, which is defined as the desired clearance plus offset distance,  $c_{des} + d_{offset}$ , then the speed-control algorithm (Yi et al., 2001) is used. The speed-control algorithm is used until the clearance becomes smaller than the transition distance, and then, if the clearance is less than the transition distance, the distance-control algo-

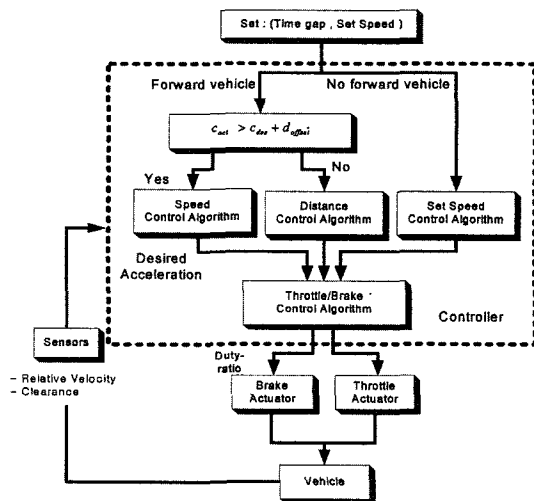


Fig. 2 Vehicle longitudinal control algorithm

rithm is used for the computation of the desired vehicle acceleration. Control inputs to the throttle/brake actuators are determined by the throttle/brake control algorithm so that the vehicle acceleration tracks the desired acceleration as closely as possible.

In order to incorporate the effect of the tire-road friction on the vehicle braking distance and the driving pattern of a driver into the headway distance, the scaled desired clearance,  $c_{des}$ , has been defined as follows :

$$c_{des} = f(\mu) \cdot q(driver) \cdot c_0 \quad (1)$$

$$c_0 = v_f t_g + d_0 \quad (2)$$

where  $f(\cdot)$  is the friction scaling function (Yi et al., 1999),  $\mu$  the tire-road friction coefficient,  $q(\cdot)$  the driver scaling function,  $v_f$  the velocity of the forward vehicle,  $t_g$  the time gap, and  $d_0$  a clearance offset. The driver scaling function must be bounded if it is desired to limit driver influence,  $q_{min} < q(\cdot) < q_{max}$ .

### 3. Vehicle Longitudinal Control Law

A two-step design approach has been used in the design of the vehicle longitudinal control algorithm. Firstly, the desired acceleration has been designed based on the distance control algorithm. Secondly, the throttle/brake control laws were designed so that the actual vehicle acceleration tracks the desired acceleration profile.

#### 3.1 Design of the desired acceleration

If there is no forward vehicle in front of the subject vehicle, the set-speed-control algorithm is chosen and the desired acceleration has been designed using a simple proportional control so that the subject vehicle speed tends to the set speed,  $v_{set}$ , as follows :

$$a_{des} = K(v_{set} - v_s) \quad (3)$$

where  $K$  is a gain and the set speed,  $v_{set}$ , has been determined by the driver.

In cases where the clearance is greater than the scaled desired clearance,  $c_{des}$ , plus the offset distance,  $d_{offset}$ , the desired acceleration has been

designed also using Eq. (3) but the set speed,  $v_{set}$ , has been defined as follows :

$$v_{set} = v_f + v_{offset} \quad (4)$$

In order to guarantee that the speed control mode changes to the distance control mode in a finite time, the set speed represented in Eq. (4) has been used. It should be noted that although a simple PI control without the offset speed,  $v_{offset}$ , guarantees that the subject vehicle speed converges to the forward vehicle speed, it does not guarantee that the clearance becomes less than the scaled desired clearance,  $c_{des}$ , plus the offset distance,  $d_{offset}$ , in a finite time.

$v_{offset}$  of 5 km/h has been used in this study. The offset values should be tuned based on vehicle tests. The gain  $K$  has been tuned to limit the jerk of the subject vehicle, and 0.8 has been used in this study.

Linear optimal control theory has been used to design the desired acceleration in the case of the distance-control mode. A state space model for the subject and forward vehicles can be written as follows :

$$\begin{aligned} \dot{x} &= Ax + Bu + \Gamma w \\ &= \begin{bmatrix} 0 & -1 \\ 0 & 0 \end{bmatrix} x + \begin{bmatrix} 0 \\ -1 \end{bmatrix} u + \begin{bmatrix} b \cdot t_g \\ 1 \end{bmatrix} w \end{aligned} \quad (5)$$

where  $b = f(\mu) \cdot g(driver)$ . The states are  $x^T = [x_1 \ x_2] = [c_{des} - c_{act} \ v_f - v_c]$ , the input,  $u$ , is the subject vehicle acceleration, and the disturbance,  $w$ , is the forward vehicle acceleration.  $c_{act}$  is the clearance between the forward and subject vehicles and  $v$  indicates velocity. Subscripts,  $f$  and  $c$ , indicate the forward and the subject vehicles, respectively. The gains for the state feedback law,  $u = -k \cdot x$ , are chosen to minimize the cost function :

$$J = \int_0^{\infty} (x^T Q x + u^T R u) dt \quad (6)$$

The weighting matrices,  $Q$  and  $R$ , are defined as follows :

$$Q = \begin{bmatrix} \rho_1 & 0 \\ 0 & \rho_2 \end{bmatrix}, R = [r] \quad (7)$$

The weighting factors,  $\rho_1$ ,  $\rho_2$  and  $r$ , are chosen to obtain a tradeoff between performance and ride comfort. The weighting factors have been

tuned based on computer simulations and vehicle test results, and  $\rho_1=1$ ,  $\rho_2=3$ , and  $r=4$  have been used in this study.

In the case of a cut-in vehicle, the control law,  $u = -k \cdot x$ , demands large, uncomfortable accelerations. In order to avoid large accelerations, which deteriorate ride comfort, the desired acceleration,  $a_{des}$ , has been obtained using a saturation function and a second order filter as follows :

$$\frac{a_{des}}{u_{sat}} = \frac{\omega^2}{s^2 + 2\zeta \cdot \omega \cdot s + \omega^2} \quad (8)$$

$$u_{sat} = sat(u) = \begin{cases} u_{max} & \text{if } u \geq u_{max} \\ u & \text{if } u_{min} < u < u_{max} \\ u_{min} & \text{if } u \leq u_{min} \end{cases} \quad (9)$$

The filter damping ratio,  $\zeta$ , of 1 and the cutoff frequency,  $\omega$ , of 5 have been used.  $u_{min}$  of  $-4.5$  m/sec<sup>2</sup> and  $u_{max}$  of 1 m/sec<sup>2</sup> have been used to provide comfortable ride quality and to avoid a kick-down of the automatic transmission during vehicle acceleration. This approach can saturate the vehicle jerk and acceleration at some maximum values.

### 3.2 Throttle/brake control law

A throttle control law has been derived under a no-slip condition of the driving wheels. At a low level of acceleration, wheel slip is quite small. The no-slip assumption has been incorporated in previous throttle/brake control designs for vehicle longitudinal control in Intelligent Cruise Control or in Automated Highways (Chang, 1994; Venhovens et al., 2000; Winner et al., 1996). Compared with a case of the ICC, the torque converter pump and turbine speed ratio varies significantly in low-speed and stop-and-go driving situations and the torque converter (Yi et al., 2000) plays an important role in those cases. A torque converter consists of a pump, a turbine and a stator. The converter pump is attached to the engine and turns at engine speed. The pump works as a centrifugal pump and the induced oil flow transfers the engine torque to the turbine. Therefore, torque converter dynamics should be considered in the development of the throttle control law.

Figure 3 shows a switching line with boundary

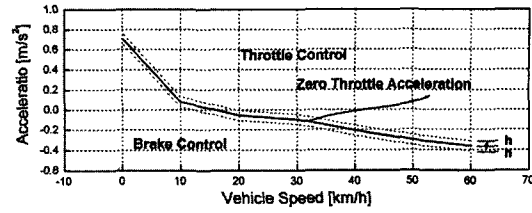


Fig. 3 Throttle/brake switching line

layer. The switching line indicates the vehicle acceleration (the minimum acceleration,  $a_{min}$ ) when the throttle is closed ( $\alpha=0$ ) for a given vehicle speed. The S&G system applies throttle control when  $a_{des} \geq a_{min} + h$  or brake control when  $a_{des} \leq a_{min} - h$  for a given vehicle speed. A switching logic with the boundary layer is necessary to avoid frequent switching between throttle and brake controls.

A block diagram of the throttle control law is shown in Fig. 4. When the desired acceleration,  $a_{des}$ , for a given vehicle velocity is greater than the throttle/brake switching line (Germann et al., 1995), i.e., the throttle control region, the desired turbine torque of the transmission,  $T_{t,des}$ , is computed from the equations of motions for the vehicle as follows :

$$\begin{aligned} T_{t,des} &= R_g T_{s,des} \\ &= R_g \cdot r \cdot [M_v (a_{des} + K_p e_a \\ &\quad + K_i \int e_a dt) + \hat{F}_L] \end{aligned} \quad (10)$$

$$e_a = a_{des} - a$$

where  $R_g$  is the gear ratio from the turbine to the wheels,  $T_{s,des}$  the desired shaft torque of the driving axle shaft,  $r$  the effective tire radius,  $M_v$  the vehicle mass,  $K_p$  and  $K_i$  gains,  $a$  the actual acceleration of the vehicle, and  $\hat{F}_L$  the estimated driving resistance load.

The desired engine speed,  $\omega_{e,des}$ , is computed from the desired turbine torque,  $T_{t,des}$ , using a torque converter map as follows :

$$\omega_{e,des} = TCM^{-1}(\omega_t, T_{t,des}) \quad (11)$$

where  $TCM^{-1}$  indicates inverse torque converter map. The torque converter map can be obtained from torque converter test results and is provided by torque converter manufacturers. It provides relationships between the turbine torque,  $T_t$ , the

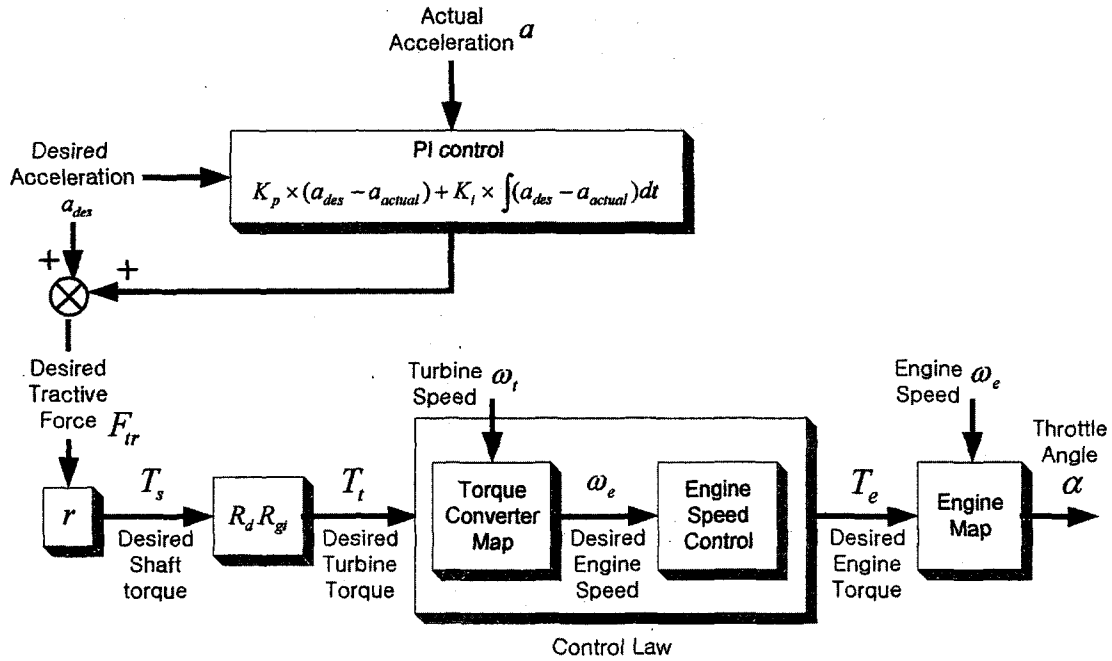


Fig. 4 Throttle control algorithm

pump torque,  $T_p$ , the pump speed,  $\omega_p$ , which is identical to the engine speed,  $\omega_e$ , and the turbine speed,  $\omega_t$ , as follows:

$$T_t = TCM(\omega_e, \omega_t) \quad (12)$$

The desired throttle angle for the desired engine speed,  $\omega_{e,des}$ , is computed from the desired net engine torque,  $T_{net,des}$ , using the engine map as follows:

$$\begin{aligned} \alpha_{des} &= EM^{-1}(\omega_e, T_{net,des}) \\ T_{net,des} &= T_p(\omega_e, \omega_t) + K_e(\omega_e, \omega_e - \omega_e) \end{aligned} \quad (13)$$

where  $EM^{-1}$  is inverse engine map and  $K_e$  the gain. Typically the engine map is given by the engine manufacturer as a lookup table. Since engine dynamics are represented as follows:

$$J_e \frac{d\omega_e}{dt} = T_{net}(\omega_e, \alpha) - T_p(\omega_e, \omega_p) \quad (14)$$

The resulting engine dynamics are represented by

$$\tau \frac{d\omega_e}{dt} + \omega_e = \omega_{e,des} \quad (15)$$

where  $\tau (= \frac{J_e}{K_e})$  is the time constant.

It has been recognized that the control law with large gains results in very jerky driving behavior due to the torque production delay of the engine.

The gain,  $K_e$ , has been tuned to obtain good acceleration tracking performance.

The brake torque is applied only when the engine braking is not sufficient to follow the desired acceleration. When the desired acceleration for a given vehicle velocity is smaller than the switching line, i.e., the brake control region, the desired brake torque,  $T_{b,des}$ , is computed from the equations of motion of the vehicle as follows:

$$\begin{aligned} T_{b,des} &= -r(M_v(a_{des} + K_p e_a + K_i \int e_a dt) \\ &\quad + \hat{F}_L) + T_s \end{aligned} \quad (16)$$

The shaft torque,  $T_s$ , is computed using the torque converter map as follows:

$$T_s = \frac{1}{R_g} TCM(\omega_e, \omega_t) \quad (17)$$

Since the total brake torque is proportional to the brake pressure, it has been assumed that the desired brake pressure,  $p_{w,des}$ , can be obtained by the equation

$$p_{w,des} = \frac{1}{K_b} T_{b,des} \quad (18)$$

where  $K_b$  is the lumped gain for the entire brake system.  $K_b$  lumps all the uncertainties in the brake

model from the brake pressure to the brake torque. The parameter,  $K_b$ , has been obtained from experimental data. A value of  $K_b=850 \text{ Nm/Pa}$  was used and it provides a good fit to one set of the experimental results. Since the brake line pressure is equal to the brake master cylinder pressure at low frequency actuation, the desired master cylinder pressure,  $p_{mc,des}$ , is set to be the brake pressure. Since the master cylinder pressure is directly connected to the vacuum booster, the desired vacuum booster pressure is given by

$$p_{d,des} = \frac{A_{mc}}{A_d} p_{mc,des} = \frac{A_{mc}}{A_d} p_w = \frac{A_{mc}}{A_d} \frac{1}{K_b} T_b \quad (19)$$

where  $A_{mc}$  is the area of the master cylinder and  $A_d$  the area of the diaphragm of the vacuum booster. Since the brake pressure is controlled at a low frequency range in a subject vehicle, the inertial effect of the connecting rod between the master cylinder and the vacuum booster is not significant. Therefore the simplified Eqs. (16), (17) and (18) represent accurately the brake system in the case of vehicle-to-vehicle distance control. It has been assumed that the differential pressure of the vacuum booster can be controlled.

#### 4. Vehicle Test Results

Vehicle tests have been conducted using a test vehicle, a 2000cc passenger car equipped with a radar distance sensor, throttle/brake actuators and a controller. The vehicle considered in this study, a radar sensor, throttle and brake actua-

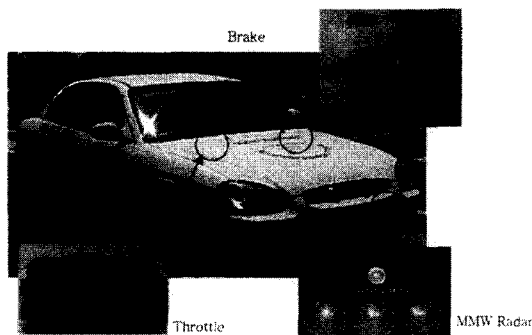


Fig. 5 Test vehicle equipped with a controller, a MMW radar sensor, a brake actuator and a throttle actuator

tors are shown in Fig. 5. The vehicle is equipped with a Millimeter Wave (MMW) radar distance sensor, a controller, a solenoid-valve-controlled Electronic-Vacuum-Booster (EVB) and a stepper motor controlled throttle actuator.

##### 4.1 Forward vehicle following

Forward vehicle following tests have been done using two vehicles : a subject vehicle and a forward vehicle. Test results are shown in Fig. 6. A comparison of vehicle speeds is shown in Fig. 6 (a). Desired and actual clearances are compared in Fig. 6(b). Both vehicles were at rest until 3 seconds and initial clearance was approximately 12.5 m. In this test, the clearance offset was set to be 5 m. Since the clearance is more than the desired clearance plus the distance offset until 6 seconds, the speed control algorithm has been chosen to make the clearance converge to the desired clearance. After 6 seconds, the control mode has been transferred from the speed control to the distance control without a large acceleration or jerk. The desired and actual accelerations of the subject vehicle are compared in Fig. 6(c). The desired acceleration has been computed so that the difference between the desired and actual clearances and relative speed are kept as small as possible without violating the acceleration constraint. The controller activates the throttle and brake actuators in order that the vehicle acceleration tracks the desired acceleration. It is illustrated that the vehicle acceleration tracks the desired one very closely. A throttle position sensor (TPS) has been used for the measurement of the throttle angle of the engine. The time histories of the throttle angle and differential pressure of the EVB are shown in Fig. 6(d) and (e), respectively. The differential pressure sensor outputs 8 bit digital values and it shows an offset of 9 [1/256 bar]. As shown in the Fig. 6(a), the forward vehicle speed varies between zero and twenty kilometers per an hour and the subject vehicle speed is close to the forward vehicle speed. It has been shown in Fig. 6(b) that the difference between the desired and actual clearances quickly decreases and the actual clearance is very close to the desired one after 10 seconds.

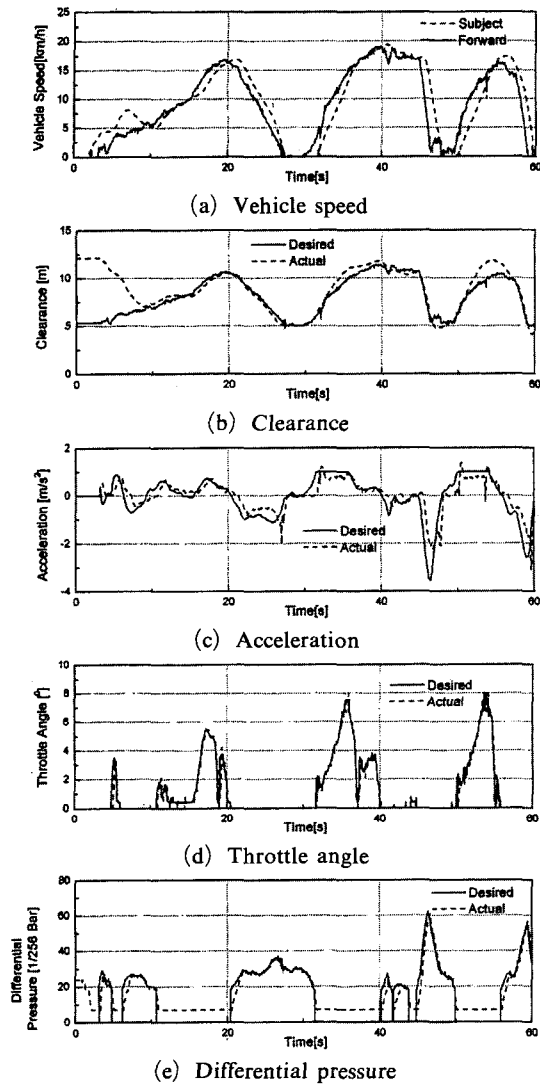


Fig. 6 Test results for a forward vehicle following case

#### 4.2 A cut-in situation

Figure 7 shows the test results for a low-speed driving situation with a cut-in vehicle. In this test, the clearance offset was set to be 2 m. 1.2 seconds of time gap has been used in this cut-in test. The initial vehicle speed was 40 km/h and a cut-in vehicle with a speed of 40 km/h has appeared in front of the subject vehicle at 6.5 seconds. The initial clearance,  $d_{ci}$ , between the subject and the cut-in vehicles was about 10 meters. The vehicle speeds and clearances are compared in Fig. 7(a) and (b), respectively. Vehicle accelerations are

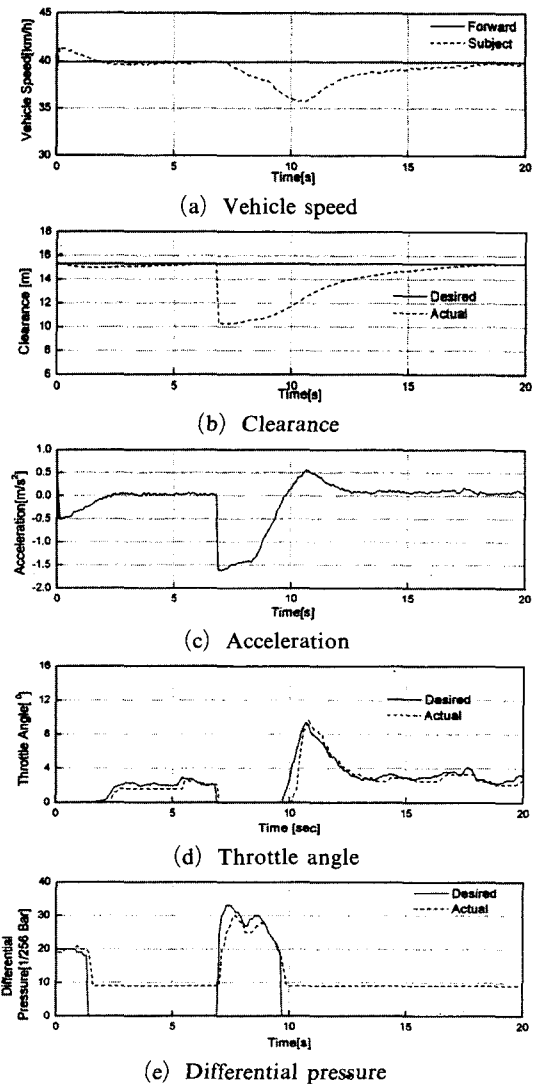


Fig. 7 Test results for a cut-in vehicle case

shown in Fig. 7(c). The desired and actual throttle angles are shown in Fig. 7(d). Comparisons of the desired and actual differential pressures of the EVB are shown in Fig. 7(e). As indicated in the figures, throttle angle was set to be zero and brakes were applied at first when the cut-in vehicle appeared to reduce the vehicle speed and to increase the clearance. And then, the controller activates the throttle actuator to increase the subject vehicle speed again so that the relative velocity converges to zero. As illustrated in Fig. 7(a) and (b), the subject vehicle speed and the clearance converge smoothly to the forward vehicle

speed and the desired clearance, respectively. The actual differential pressure of the EVB shows sensor offset when the brake command is not applied.

**4.3 A set-speed-control situation**

Test results for a set-speed driving situation, no vehicle in front of the subject vehicle, are presented in Fig. 8. The vehicle speed and set-speed, which has been set by the driver, are shown in Fig. 8(a). It has been shown that the vehicle actual speed is very close to the desired set-speed. The desired and actual accelerations of the subject vehicle are compared in Fig. 8(b). The actual acceleration tracks the desired acceleration closely. The desired and actual throttle angles are shown in Fig. 8(c). Comparisons of the desired and actual differential pressures are shown in Fig. 8(d). In the case where the set-speed is

20 km/h, braking is not necessary and only the throttle control has been used to control the vehicle speed. It should be noted that the desired differential pressure is zero during set-speed-control and the non-zero values of the actual differential pressure are the sensor offset.

**5. Conclusions**

A vehicle longitudinal control scheme for stop-and-go cruise control, vehicle test results have been presented. The vehicle control algorithm consists of a distance control algorithm and resulting throttle/brake control laws. It has been shown that the proposed control algorithm can provide good distance control performance over the vehicle modeling errors such as the engine map data error and the torque converter model errors. This is promising since the engine and torque converter characteristics are time varying depending on driving conditions. Vehicle test results show that the control scheme seems suitable for Stop and Go cruise control systems. It can be concluded from the vehicle test results that the proposed control algorithm can be used for Stop and Go cruise control systems to reduce the workload of the driver in a congested traffic flow.

**Acknowledgment**

This work was jointly supported by Grant No. R01-2000-000-00301-0 from the Basic Research Program of the Korea Science and Engineering Foundation and the national project (G7) through the Korea Automotive Technology Institute (KATECH).

**References**

Chang, A. T. S., 1994, "ADVANCE-F's Car Following Policy on Vehicle Cruise and Automatic Speed Control," *Intelligent Vehicles '94 Symposium, Paris, IEEE Industrial Electronics Society*, pp. 498~503.  
 Chien, C. C., Ioannou, P. and Lai, M. C., 1994, "Entrainment and Vehicle Following Controllers Design for Autonomous Intelligent Vehicles,"

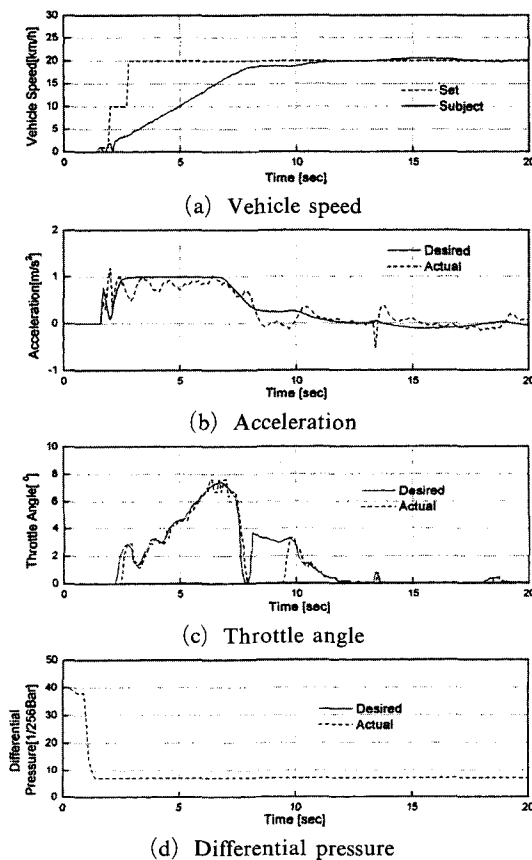


Fig. 8 Test results for a set-speed case



- Proceedings of the 1994 American Control Conference*, Baltimore, Maryland, pp. 6~10.
- Cho, D. and Hedrick, J. K., 1989, "Automotive Powertrain Modeling for Control," *ASME Transactions on Dynamic System, Measurements and Control*, Vol. 111.
- Choi, S. and Devlin, P., 1995, "Throttle and Brake Combined Control for Intelligent Vehicle Highway Systems," SAE paper No. 951897.
- Fenton, R. E. and Bender, J. G., 1969, "A Study of Automatic Car Following," *IEEE Trans. On Vehicle Tech.* VT-18(3).
- Fujioka, T., Aso, M. and Baba, J., 1995, "Comparison of Sliding and PID Control for Longitudinal Automated Platooning," *Systems and Issues in ITS*, pp. 61~67.
- Germann, St. and Isermann, R., June 1995, "Nonlinear Distance and Cruise Control for Passenger Cars," *Proceedings of the 1995 American Control Conference*, Seattle, Washington, pp. 3081~3085.
- Hedrick, J. K., McMahon, D., Narendra, V. and Swaroop, D., 1991, "Longitudinal Vehicle Controller Design for IVHS Systems," *Proceedings of the 1991 American Control Conference*, Boston, Massachusetts, pp. 3107~3112.
- Hedrick, J. K., 1993, "Longitudinal Control and Platooning," In *TOPTEC: Collision Avoidance Systems for Intelligent Vehicles*, Washington, D. C., SAE.
- Hoess, A., Hosp, W., Doerfler, R. and Rauner, H., 1996, "Longitudinal Autonomous Vehicle Control Utilizing Access to Electronic Throttle Control, Automatic Transmission and Brakes," SAE paper No. 961009.
- Ioannou, P., Xu, Z., Eckert, S., Clemons, D. and Sieja, T., 1993, "Intelligent Cruise Control: Theory and Experiment," *Proceedings of the 32<sup>nd</sup> Conference on Decision and Control*, volume 2, San Antonio, Texas, pp. 1885~1890.
- Muller, R. and Nocker, G., 1992, "Intelligent Cruise Control with Fuzzy Logic," *In Intelligent Vehicles '92 Symposium, Detroit, IEEE Industrial Electronics Society*, pp. 173~178.
- Rajamani, R., Choi, S. B., Hedrik, J. K. and Law, B., 1998, "Design and Experimental Implementation of Control for a Platoon of Automated Vehicles," *Proc. of the ASME Dynamic Systems and Control Division, ASME*, pp. 681~689.
- Shladover, S. E., 1978, "Longitudinal Control of Automotive Vehicles in Close-Vehicle Formation Platoons," *JDSMC 100*, pp. 302~310.
- Venhovens, P., Naab, K. and Adiprasito, 2000, "Stop and Go Cruise Control," *Seoul 2000 FISITA World Automotive Congress*, Seoul, Korea.
- Winner, H., Witte, S., Uhler, W. and Litchtenberg, B., 1996, "Adaptive Cruise Control System Aspects and Development Trends," SAE paper No. 961010.
- Yi, K., Woo, M., Kim, S. and Lee, S., 1999, "A Study on a Road-Adaptive CW/CA Algorithm for Automobiles Using HiL Simulations," *JSME International Journal, Series C*, Vol. 42, No. 1, pp. 163~170.
- Yi, K., Shin, B. and Lee, K. I., June 2000, "Estimation of Turbine Torque of Automatic Transmissions Using Nonlinear Observers," *ASME Trans. J. of Dynamic Systems, Measurement, and Control*, Vol. 122, No. 2, pp. 276~283.
- Yi, K. Lee, S. and Lee, J., 2000, "Modeling and Control of an Electronic-Vacuum Booster for Vehicle-to-Vehicle Distance Control," *Proceedings of AVEC 2000, 5<sup>th</sup> International Symposium on Advanced Vehicle Control*, 2000, pp. 7~14.
- Yi, K., Lee, S. and Kwon, Y. D., 2001, "An Investigation of Intelligent Cruise Control Laws for Passenger Vehicles," *Proceedings of the Institution of Mechanical Engineers, Part D*, 2001, Vol. 215, No. D2, pp. 159~169.